

## Article

# Multi-Objective Disassembly Depth Optimization for End-of-Life Smartphones Considering the Overall Safety of the Disassembly Process

Zepeng Chen, Lin Li <sup>\*</sup>, Xiaojing Chu, Fengfu Yin and Huaqing Li

College of Electromechanical Engineering, Qingdao University of Science and Technology, Qingdao 266061, China; 2021030005@mails.qust.edu.cn (Z.C.); 4022030010@mails.qust.edu.cn (X.C.); yinff@qust.edu.cn (F.Y.); 4021030017@mails.qust.edu.cn (H.L.)

\* Correspondence: ll@qust.edu.cn

**Abstract:** The disassembly of end-of-life (EoL) products is of high concern in sustainability research. It is important to obtain reasonable disassembly depth during the disassembly process. However, the overall safety of the disassembly process is not considered during the disassembly depth optimization process, which leads to an inability to accurately obtain a reasonable disassembly depth. Considering this, a multi-objective disassembly depth optimization method for EoL smartphones considering the overall safety of the disassembly process is proposed to accurately determine a reasonable disassembly depth in this study. The feasible disassembly depth for EoL smartphones is first determined. The reasonable disassembly process for EoL smartphones is then established. A multi-objective function for disassembly depth optimization for EoL smartphones is established based on the disassembly profit per unit time, the disassembly energy consumption per unit time and the overall safety rate of the disassembly process. In order to increase solution accuracy and avoid local optimization, an improved teaching-learning-based optimization algorithm (ITLBO) is proposed. The overall safety of the disassembly process, disassembly time, disassembly energy consumption and disassembly profit are used as the criteria for the fuzzy analytic hierarchy process (AHP) to evaluate the disassembly depth solution. A case of the 'Xiaomi 4' smartphone is used to verify the applicability of the proposed method. The results show that the searchability of the non-inferior solution and the optimal solution of the proposed method are improved. The convergence speeds of the ITLBO algorithm are 50.00%, 33.33% and 30.43% higher than those of the TLBO algorithm, and the optimal solution values of the ITLBO algorithm are 3.91%, 5.10% and 3.45% higher than those of the TLBO algorithm in three experiments of single objective optimization.

**Keywords:** disassembly depth; overall safety of disassembly process; ITLBO algorithm; Fuzzy AHP



**Citation:** Chen, Z.; Li, L.; Chu, X.; Yin, F.; Li, H. Multi-Objective Disassembly Depth Optimization for End-of-Life Smartphones Considering the Overall Safety of the Disassembly Process. *Sustainability* **2024**, *16*, 1114. <https://doi.org/10.3390/su16031114>

Academic Editor: Khampheng Phoungthong

Received: 22 December 2023

Revised: 23 January 2024

Accepted: 26 January 2024

Published: 28 January 2024



**Copyright:** © 2024 by the authors. Licensee MDPI, Basel, Switzerland. This article is an open access article distributed under the terms and conditions of the Creative Commons Attribution (CC BY) license (<https://creativecommons.org/licenses/by/4.0/>).

## 1. Introduction

The rapid development of science and technology has accelerated the speed of product updates and shortened the service life of products, resulting in a large number of end-of-life (EoL) products such as televisions and personal computers [1]. According to statistics, China produces nearly 10 million EoL smartphones every year [2] and the recycling rate for EoL smartphones in China is less than 1% [3]. Because these EoL products have not been properly treated, the accumulation of waste products results. The accumulation of waste products threatens the natural environment and wastes a lot of resources [4]. Recycling, reusing and remanufacturing EoL products not only allows the recycling of resources but also reduces environmental pollution and increases economic benefits [5]. Disassembly is a crucial step in the recycling and remanufacturing process and plays an irreplaceable role in sustainable development [6]. By analyzing the existing research, it can be seen that the partial disassembly mode is more practical than the complete disassembly mode [7].

Therefore, the partial disassembly mode has been widely accepted and adopted by disassembly enterprises [8]. However, how to reasonably secure a satisfactory disassembly depth to improve efficiency and reduce costs has always been a concern for enterprises and researchers.

As one of the prevalent and short-life (the average lifespan of a mobile phone is only 3.17 years) electrical and electronic equipment [9,10], the disassembly depth optimization problem of EoL smartphones has attracted increasing attention. At present, there are multiple studies focusing on electrical and electronic equipment wastes in terms of economic benefits and environmental impact [11,12]. In the actual disassembly process, disassembly safety is particularly important. In terms of disassembly safety, the traditional disassembly mode only focuses on the disassembly safety of some parts with high disassembly risk. To the best of our knowledge, the overall disassembly safety process that is more in line with actual production is not considered during the disassembly depth optimization process, which leads to an inability to accurately obtain a reasonable disassembly depth. Therefore, research on the disassembly depth optimization problem of EoL smartphones, considering the overall disassembly safety process, makes sense in both theoretical and practical aspects.

Given this background, a multi-objective disassembly depth optimization method for EoL smartphones considering the overall safety of the disassembly process is proposed in this work. In comparison with existing studies, this paper makes the following contributions:

- (1) A multi-objective function for disassembly depth optimization of EoL smartphones is established based on disassembly profit per unit time, disassembly energy consumption per unit time and overall safety rate of the disassembly process.
- (2) An improved teaching–learning-based optimization algorithm (ITLBO) is proposed with an improved teacher phase for increasing the solution accuracy and increasing the singer chaotic map to avoid local optimization.
- (3) The overall safety of the disassembly process, disassembly time, disassembly energy consumption and disassembly profit are selected as the criteria for the fuzzy analytic hierarchy process (AHP) to obtain the optimal disassembly depth for EoL smartphones.

The rest of this paper is organized as follows: Section 2 reviews the relevant literature. In Section 3, a multi-objective disassembly depth optimization method for EoL smartphones considering the overall disassembly safety process is introduced. Section 4 analyzes EoL smartphone disassembly as an illustrative example. Section 5 concludes this paper and indicates future research issues.

## 2. Literature Review

During the disassembly optimization process, the objective function is established considering the different disassembly factors. The disassembly model is an intuitionistic method for expressing the disassembly factors. Ren et al. [13] used disassembly profit as the objective function for the partial disassembly line balancing problem. Mandolini et al. [14] assessed the best disassembly time for target components using the disassembly time model. Yang et al. [15] proposed the objective function of the disassembly line balancing problem based on the disassembly time model, the carbon dioxide emissions model and the recycling cost model. Time efficiency, energy efficiency and value efficiency are newly defined by Cao et al. [16] as optimization objectives. Lu et al. [17] proposed that profit and energy consumption should be considered as important criteria. Xu et al. [18] adopted disassembly time, disassembly cost and disassembly difficulty to evaluate the generated disassembly solution. Xing et al. [19] used the disassembly time model to consider execution time and preparation time to solve the asynchronous parallel disassembly sequence planning problem. Liu et al. [20] formulated a profit model to plan the disassembly sequence. Liang et al. [21] proposed the energy consumption model for disassembly activities for a two-sided disassembly line balance. In order to choose the best and most feasible

disassembly plan, Aicha et al. [22] proposed a mathematical formulation that combines the index of quality and the index of processing time. Zeng et al. [23] established the energy consumption and profit-oriented multi-product disassembly line balancing model. Wang et al. [24] constructed the comprehensive optimization objectives model that includes minimizing the number of stations and smoothness index, maximizing disassembly profit and minimizing disassembly energy consumption. The above researchers took disassembly profit, disassembly time and environmental impacts as the disassembly optimization objectives. However, the overall safety of the disassembly process is not reasonably considered in the existing research; therefore, a multi-objective function that quantifies the overall safety of the disassembly process should be established to provide guidance for disassembly depth optimization for EoL smartphones.

In the existing literature, research on the disassembly optimization problem for EoL products mainly focuses on the solution methods. During the process of handling EoL products, Yeh et al. [25] proposed the use of the modified simplified swarm optimization algorithm to seek the optimal disassembly sequence. Xia et al. [26] presented a simplified teaching-learning-based optimization algorithm for solving disassembly sequence planning problems effectively. As the complexity of products increases, Tseng et al. [27] presented a block-based genetic algorithm for disassembly sequence planning to improve the solution quality. As the size of components increases, Xie et al. [28] proposed a modified grey wolf optimizer to obtain the optimal disassembly sequence. Tseng et al. [29,30] used a Flatworm algorithm and an improved particle swarm optimization algorithm to optimize the disassembly sequence. Lou et al. [31] proposed an improved multi-objective hybrid grey wolf optimization algorithm to obtain Pareto optimal disassembly plans. Kalayci et al. [32] proposed a hybrid genetic algorithm for the sequence-dependent disassembly line balancing problem. Considering the disassembly precedence relationships and sequence-dependent parts removal time increments, Liu et al. [33] presented an improved discrete artificial bee colony algorithm for solving the sequence-dependent disassembly line balancing problem. Liu et al. [34] designed an improved multi-objective discrete bee algorithm to solve the problem of robot disassembly line balancing. Xia et al. [35] proposed an improved adaptive simulated annealing genetic algorithm to balance the disassembly line. Xu et al. [36] proposed the improved discrete bee algorithm to obtain the optimal solution for the human-robot collaborative disassembly line balancing problem. Liang et al. [37] devised a multi-objective group teaching optimization algorithm to solve the disassembly line balancing problem. In order to improve the ease of disassembly, Giudice et al. [38] introduced a structured method for the analysis and reconfiguration of the disassembly depth. Achillas et al. [39] presented a mathematical formulation based on the cost-benefit analysis concept to determine the optimal disassembly depth for a given product. Smith et al. [40] used life cycle impact assessment tools (Simapro Eco-indicator 99) to perform cost-benefit analyses to find an optimized disassembly depth. At present, heuristic optimization algorithms with excellent performance are used for disassembly optimization by a majority of researchers. However, heuristic optimization algorithms are almost not used in the study of the disassembly depth optimization problem. This leads to difficulties in obtaining an accurate optimal disassembly depth for EoL products. Therefore, heuristic optimization algorithms with excellent performance are important for the disassembly depth optimization process.

The selection of the optimal scheme from many non-inferior schemes is difficult. As a method with reliable performance, the fuzzy AHP was used in a related study [41]. Because different products have different features, the criteria for the fuzzy AHP are also different [42]. Heo et al. [43] proposed five criteria (technological, market-related, economic, environmental and policy-related) for evaluating the renewable energy dissemination program. In order to evaluate the disassembly line balancing schemes, the task time, part demand, revenue generated, part hazardous, state of material and fragility were taken into consideration by Avikal et al. [44]. Yang et al. [15] proposed five criteria for the disassembly line balance problem as follows: workstation number, smoothness index, disassembly time,

CO<sub>2</sub> saving rate and recycling cost. Considering the selection of the fast charging station for the electric vehicle, ten related criteria (population density, shopping malls, roads, income rates, transportation stations, petrol stations, park areas, green areas, slope and land values) were proposed by Guler et al. [45]. In order to determine the optimal copper removal process, Zhou et al. [46] proposed four criteria (the total cost, stability, reaction rate and reliability) for evaluating copper removal schemes. Economic, technical, environmental and social factors were used by Sherif et al. [47] for the selection of battery recycling plant locations in sustainable environments. Tuo et al. [48] used AHP to evaluate the retention attributes of tasks based on the problem characteristics and the high-value attributes of the task (appearance and mechanical and electrical components). Disassembly time, disassembly energy consumption and disassembly profit were used by many researchers as the criteria for selecting the optimal disassembly depth for EoL smartphones. However, the overall safety of the disassembly process of EoL smartphones has been neglected. Therefore, the overall safety of the disassembly process should also be used as an important criterion for selecting the optimal disassembly depth for EoL smartphones.

The above research results have laid the foundation for research on disassembly depth optimization for EoL smartphones. However, the overall safety of the disassembly process for each disassembly depth was seldom mentioned in the above literature, which leads to an inability to accurately obtain a reasonable disassembly depth during the disassembly depth optimization process. Therefore, a multi-objective disassembly depth optimization method for EoL smartphones, considering the overall safety of the disassembly process, is proposed in this paper. We introduce this proposed method in the next section.

### 3. The Proposed Method

In this section, a multi-objective disassembly depth optimization method for EoL smartphones considering the overall safety of the disassembly process is proposed. The flow chart of the proposed method is shown in Figure 1.

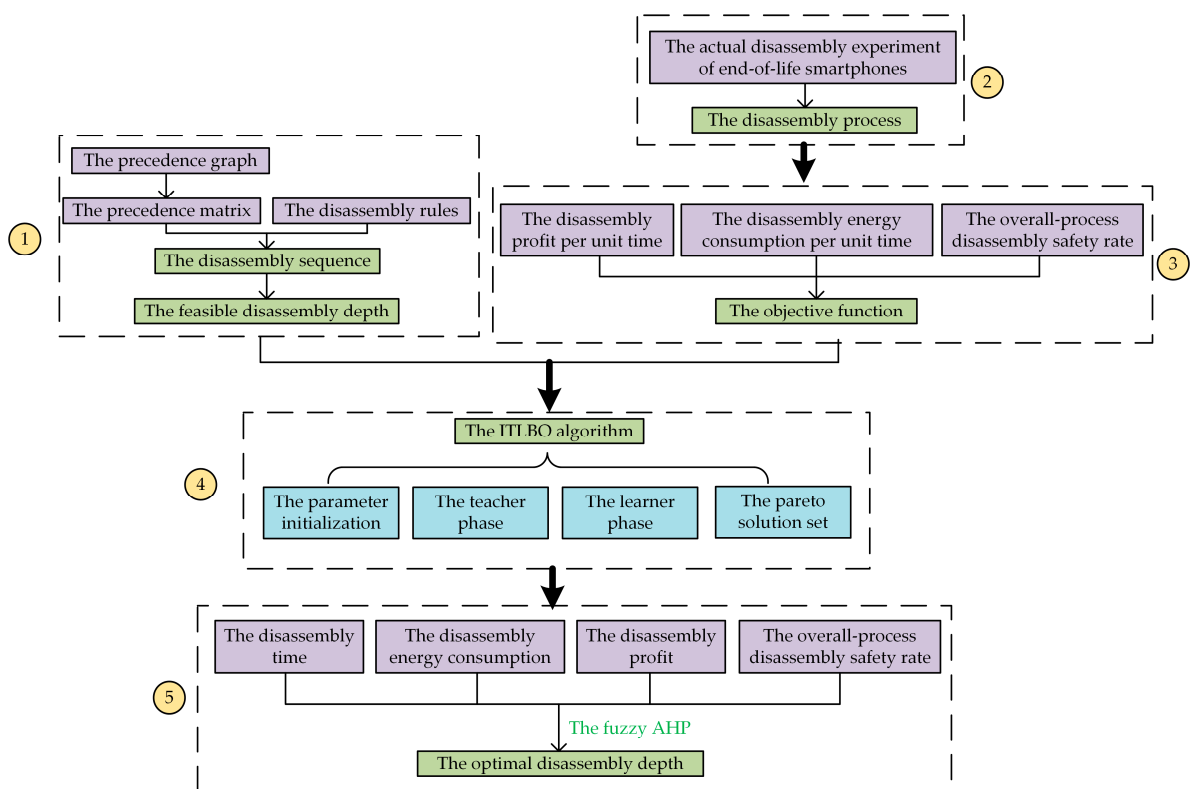


Figure 1. The flow chart of the proposed method.

In the first step, the feasible disassembly depth of the EoL smartphones is determined based on the precedence graph and disassembly rules. The second step is to establish a reasonable disassembly process. In the third step, a multi-objective function is established based on the disassembly profit per unit time, the disassembly energy consumption per unit time and the overall safety rate of the disassembly process. In the fourth step, the ITLBO algorithm is proposed to optimize the disassembly depth. The fifth step assesses the disassembly depth in the pareto solution set using fuzzy AHP.

### 3.1. Determination of the Feasible Disassembly Depth

A precedence diagram is commonly used to represent the relationships between parts of the EoL product. For example, Figure 2 shows the precedence relationship between EoL smartphone parts. The precedence constraint between two parts is connected by a unidirectional edge. The precedence matrix is obtained based on the precedence graph. For instance, part 1 is the predecessor of part 2; thus, part 1 is disassembled before part 2, and  $D_{12} = 1$ . Part 4 is not the predecessor of part 1; thus, part 4 is not disassembled before part 1, and  $D_{41} = 0$ .

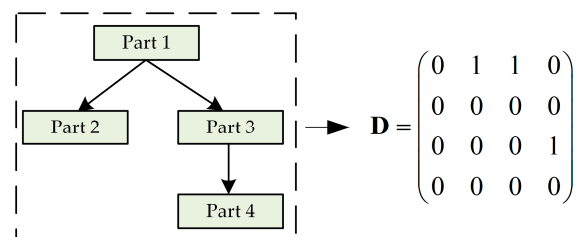


Figure 2. Precedence graph and precedence matrix.

The disassembly rules are used to obtain some optimized disassembly plans. The decision order of disassembly rules is rotated during disassembly sequence planning. The specific content of disassembly rules is as follows: (1) remove the part that has the highest economic benefit first; (2) remove the parts that can be removed in the same disassembly direction first; (3) remove the parts that use the same tool first; (4) remove the parts that change the small disassembly directions first.

The disassembly sequences are generated based on the precedence graph, the precedence matrix and the disassembly rules. Then, the feasible disassembly depth is obtained by dividing the disassembly stopping points of the above disassembly sequences. The specific process for determining the feasible disassembly depth is shown in Figure 3.

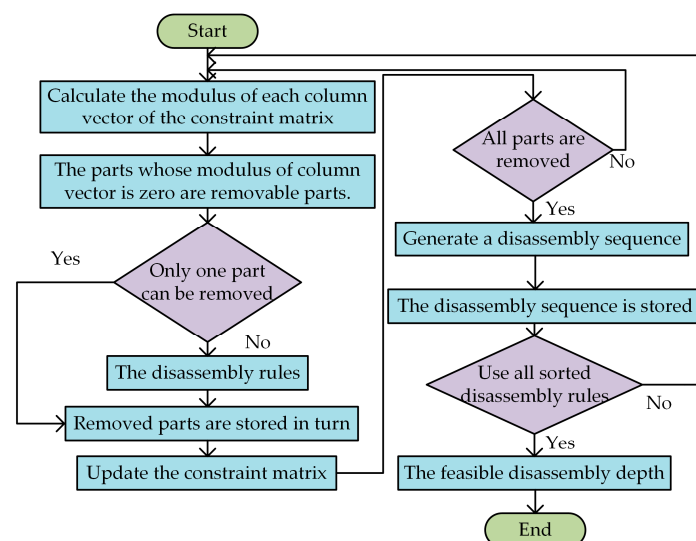


Figure 3. The process graph for determining the feasible disassembly depth.

### 3.2. Establishment of the Disassembly Process

A reasonable disassembly process can improve the accuracy of the optimization model. Thus, it is important to establish a reasonable disassembly process. In this section, the disassembly process is built by analyzing the actual disassembly experiment for EoL smartphones. The specific disassembly process for EoL smartphones is shown in Figure 4.

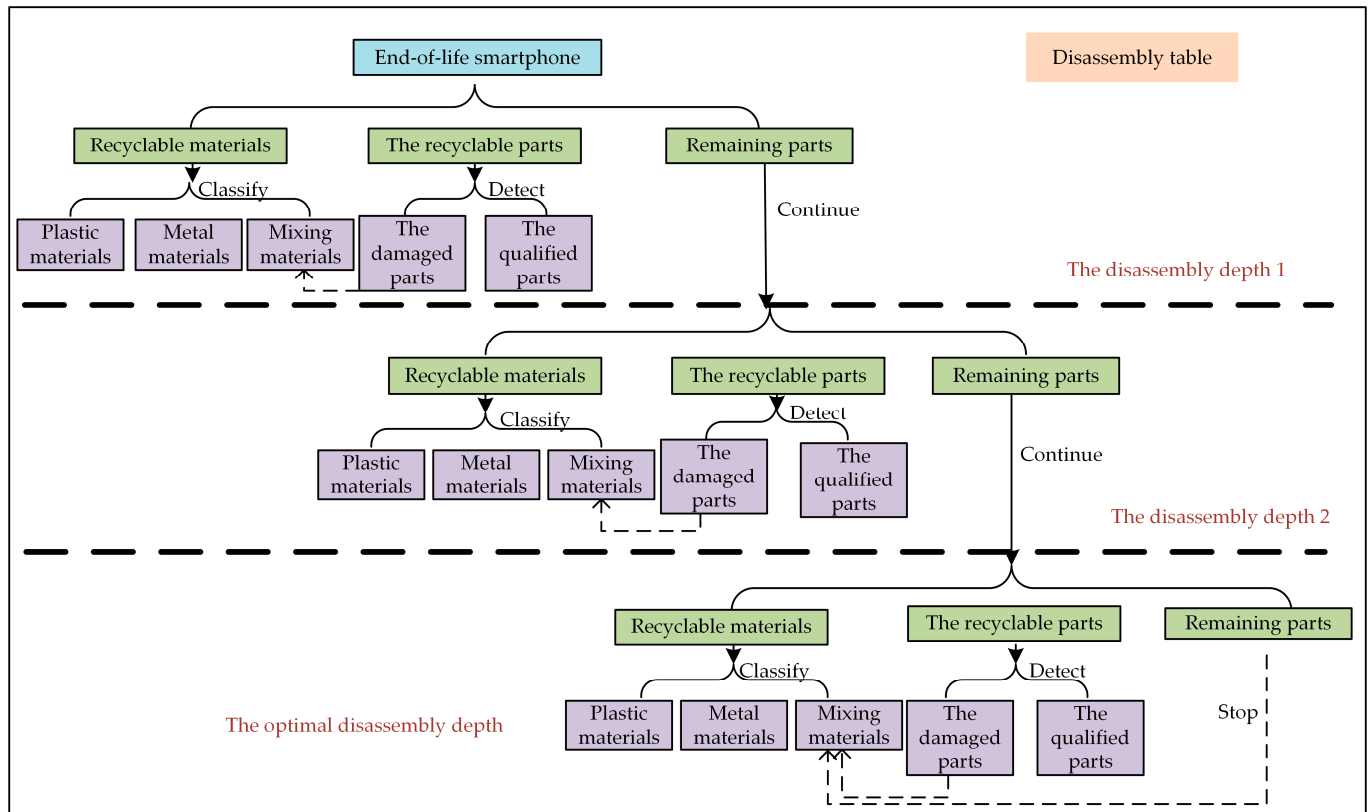


Figure 4. The disassembly process for EoL smartphones.

The EoL smartphone is divided into recyclable materials, recyclable parts and remaining parts. Recyclable materials are divided into plastic materials, metal materials and mixing materials. The recyclable parts are divided into damaged parts and qualified parts. The damaged parts are treated as mixing materials. When the current disassembly depth is not the optimal disassembly depth, the remaining parts are disassembled continuously. When the current disassembly depth is the optimal disassembly depth, the remaining parts are not disassembled. The remaining parts of the optimal disassembly depth are treated as mixing materials.

### 3.3. Establishment of Objective Function

The main factors influencing the disassembly depth are environmental impact and economic benefits. As one of the most prevalent electronic devices, the overall disassembly safety process is also a key factor in EoL smartphones. Therefore, the disassembly profit per unit time, the disassembly energy consumption per unit time and the overall safety rate of the disassembly process are selected as the objectives for evaluating the disassembly depth of EoL smartphones. For the convenience of the research, the disassembly process should meet the following assumptions: (1) The research object is an EoL smartphone (the representative of the EoL equipment) in the disassembly table. (2) Only one main part can be disassembled at each time. (3) The disassembly is in an ideal state; the parts are not damaged during the disassembly process. (4) All parts of the EoL smartphone can be recycled.

The disassembly time model for EoL smartphones mainly considers five factors as follows: the basic disassembly time (the time of the necessary disassembly action), the tool changing time, the tool positioning time, the detection time and the tidying time.

The tool changing time for disassembling part  $i$  ( $u_i$ ) is determined as follows:

$$u_i = N_i v \quad (1)$$

where  $v$  is the time required to change the disassembly tool once and  $N_i$  is the number of changing tools when part  $i$  is disassembled.

The tool positioning time for disassembling part  $i$  ( $h_i$ ) is determined as follows:

$$h_i = z_i m \quad (2)$$

where  $z_i$  is the constraint number for part  $i$  and  $m$  is the tool positioning time for removing a constraint.

The total disassembly time for disassembling an EoL smartphone ( $T$ ) is determined as follows:

$$T = \sum_{i=1}^n (f_i + N_i v + z_i m + C + J) \quad (3)$$

where  $f_i$  is the basic disassembly time for part  $i$ ,  $C$  is the tidying time for disassembling a part,  $J$  is the detection time for a part and  $n$  is the number of EoL smartphone parts.

The disassembly profit is affected by the disassembly benefit and the disassembly cost. The disassembly benefit mainly considers the benefits of recyclable materials and recyclable parts. The disassembly cost mainly considers the following factors: the procurement cost, the employee cost, the workshop rental cost, the electricity cost and the tool damaging cost.

The disassembly benefit of the recyclable parts of an EoL smartphone ( $B_1$ ) is determined as follows:

$$B_1 = \sum_{i=1}^n (r_i \times p) \quad (4)$$

where  $r_i$  is the price of recyclable part  $i$  and  $p$  is the quality rate of recyclable parts.

The disassembly benefit of recyclable materials in an EoL smartphone ( $B_2$ ) is determined as follows:

$$B_2 = Z_1 D_1 + Z_2 D_2 + Z_3 D_3 \quad (5)$$

where  $Z_1$  is the weight of the plastic materials,  $Z_2$  is the weight of the metal materials,  $Z_3$  is the weight of the mixing materials,  $D_1$  is the unit price for the plastic materials,  $D_2$  is the unit price for the metal materials and  $D_3$  is the unit price for the mixing materials.

The employee cost of disassembling an EoL smartphone ( $C_2$ ) is determined as follows:

$$C_2 = T \times \frac{k_1}{3600} \quad (6)$$

where  $k_1$  is the employee cost for an hour.

The workshop rental cost for disassembling an EoL smartphone ( $C_3$ ) is determined as follows:

$$C_3 = \frac{k_2}{d \times h \times 3600} \times \frac{T}{a} \quad (7)$$

where  $k_2$  is the workshop rental cost for a month,  $a$  is the number of disassembly tables in a workshop,  $d$  is the number of working days in a month and  $h$  is the daily working time.

The electricity cost of disassembling an EoL smartphone ( $C_4$ ) is determined as follows:

$$C_4 = \frac{(P_1 \times t_1 + P_2 \times t_2 + P_3 \times t_3 + P_4 \times t_4)}{3.6 \times 10^6} \times c \quad (8)$$

where  $P_1$  is the power of the hot air gun,  $P_2$  is the power of the electric screwdriver,  $P_3$  is the power of the detector,  $P_4$  is the power of the lamp,  $t_1$  is the working time of the hot air

gun,  $t_2$  is the working time of the electric screwdriver,  $t_3$  is the working time of the detector,  $t_4$  is the working time of the lamp and  $c$  is the price per kilowatt-hour of electricity. The units for  $P_1, P_2, P_3$  and  $P_4$  is watt.

The tool damaging cost of disassembling an EoL smartphone ( $C_5$ ) is determined as follows:

$$C_5 = \sum_{l=1}^q (u_l \times g_l) \quad (9)$$

where  $q$  is the number of tools,  $u_l$  is the time spent using the tool  $l$  and  $g_l$  is the tool damage cost of using tool  $l$  once.

The total profit of disassembling an EoL smartphone ( $L$ ) is determined as follows:

$$L = B_1 + B_2 - C_1 - C_2 - C_3 - C_4 - C_5 \quad (10)$$

where  $C_1$  is the procurement cost.

The disassembly profit per unit time of disassembling an EoL smartphone ( $L_1$ ) is determined as follow:

$$L_1 = \frac{L}{T} \quad (11)$$

Through the actual disassembly experiment and by analyzing the disassembly of EoL smartphones, we think that disassembly energy consumption mainly comes from the following five aspects: using the suction cups, moving tools and parts, disassembling the board to board (BTB) connectors, disassembling the buckle and using the electric equipment. Therefore, the disassembly energy consumption model is constructed based on the following aspects: energy consumption when using the suction cups, energy consumption by moving tools and parts, energy consumption when disassembling the BTB connectors, energy consumption for disassembling the buckle, and energy consumption when using the electric equipment.

The suction cup is only used to remove the back cover. The energy consumed when using the suction cups ( $M_1$ ) is determined as follows:

$$M_1 = F_1 \times H_1 \quad (12)$$

where  $F_1$  is the traction generated using the suction cup and  $H_1$  is the distance of moving the suction cup. The unit of measurement of  $F_1$  is Newton.

The energy consumed by moving tools and parts ( $M_2$ ) is determined as follows:

$$M_2 = \sum_{k=1}^{m_2} F_{2k} \times H_{2k} \quad (13)$$

where  $F_{2k}$  is the force of moving tools and parts  $k$ ,  $H_{2k}$  is the distance of moving tools and parts  $k$ ,  $m_2$  is the number of tools and parts and  $m_2$  is the sum of the number of tools ( $q$ ) and the number of parts ( $n$ ). The unit of measurement of  $F_{2k}$  is Newton.

The energy consumption during disassembling of the BTB connectors ( $M_3$ ) is determined as follows:

$$M_3 = \sum_{e=1}^{m_3} \frac{E_c H_{3e} t_{1e}^3 H_{4e}^2}{8 H_{5e}^3} \quad (14)$$

where  $m_3$  is the number of BTB connectors,  $E_c$  is the elastic modulus,  $H_{3e}$  is the connection position width of the BTB connector  $e$ ,  $t_{1e}$  is the connection position thickness of the BTB connector  $e$ ,  $H_{4e}$  is the height of the BTB connector  $e$  and  $H_{5e}$  is the length of the connector  $e$ .

The energy consumption during disassembling of the buckle ( $M_4$ ) is determined as follows:

$$M_4 = \sum_{f=1}^{m_4} F_{6f} \times H_{6f} \quad (15)$$

where  $m_4$  is the number of buckle  $f$ ,  $F_{6f}$  is the force of disassembling buckle  $f$  and  $H_{6f}$  is the distance of disassembling buckle  $f$ . The unit of measurement of  $F_{6f}$  is Newton.

The energy consumption when using the electric equipment ( $M_5$ ) is determined as follows:

$$M_5 = P_1 \times t_1 + P_2 \times t_2 + P_3 \times t_3 + P_4 \times t_4 \quad (16)$$

The total disassembly energy consumption when disassembling an EoL smartphone ( $M$ ) is determined as follows:

$$M = M_1 + M_2 + M_3 + M_4 + M_5 \quad (17)$$

The disassembly energy consumption per unit time of disassembling an EoL smartphone ( $M_6$ ) is determined as follows:

$$M_6 = \frac{M}{T} \quad (18)$$

By analyzing the disassembly process of EoL smartphones, we found that the temperature of the disassembly environment, the accuracy of the tool positioning, the heat dissipation performance of the disassembly tool and the risky degree of parts are the main factors influencing the disassembly safety of each part. Therefore, the model for the overall safety of the disassembly process for disassembling an EoL smartphone is constructed considering the above four factors. Four factors influencing disassembly are defined as follows: (1) The disassembly process is considered risky when the temperature of the disassembly environment is higher than 60 °C. (2) The disassembly process is considered risky when the positioning of the tool is biased. (3) The disassembly process is considered risky when the temperature of the disassembly tool is higher than 55 °C. (4) The disassembly process is considered risky when the operator is injured by the parts. The rate of risk of disassembling each part is determined using the disassembly experiment. Three operators with a similar disassembly experience are divided into three groups. The operator of every group disassembles the same part and repeats this  $W$  times. The number of risky disassembly experiments in every group is recorded.

The rate of risk of disassembling part  $i$  ( $A_i$ ) is determined as follows:

$$A_i = \frac{\left(\frac{w_{1i}}{W} + \frac{w_{2i}}{W} + \frac{w_{3i}}{W}\right)}{3} \times 100\% \quad (19)$$

where  $w_{1i}$  is the risky number of disassembling part  $i$  in the first disassembly experiment group,  $w_{2i}$  is the risky number of disassembling part  $i$  in the second disassembly experiment group and  $w_{3i}$  is the risky number of disassembling part  $i$  in the third disassembly experiment group.

The overall safety rate of the disassembly process when disassembling an EoL smartphone ( $O$ ) is determined as follows:

$$O = \prod_{i=1}^{m_5} (1 - A_i) \times 100\% \quad (20)$$

where  $m_5$  is the number of disassembling parts at each disassembly depth.

The disassembly profit per unit time, the disassembly energy consumption per unit time and the overall safety rate of the disassembly process are selected as the optimization objectives. The objective function ( $f(x)$ ) is constructed as follows:

$$\min f(x) = \min \left[ \frac{1}{O}, \frac{1}{L_1}, M_6 \right] \quad (21)$$

### 3.4. Optimization of Disassembly Depth

The TLBO algorithm is proposed based on inspiration from the teaching and learning process. Teacher and learners are the two vital components of the algorithm and describe the two basic modes of learning through the teacher phase and the learner phase. Because the TLBO algorithm is only needed to set the initial parameters and the solution process of the TLBO algorithm is simple, the TLBO algorithm is widely used. Therefore, the ITLBO algorithm is proposed for solving the multi-objective disassembly depth optimization problem of EoL smartphones in this section. In order to avoid falling into the local optimum, the Singer chaotic map is used in the population initialization of the ITLBO algorithm. In the teacher phase of the ITLBO algorithm, the nonlinear convergence factor is used to increase the searchability and solution accuracy. The Pareto solution set is used to obtain the disassembly depth that can consider multiple objectives of the EoL smartphones. The flow chart of the ITLBO algorithm is shown in Figure 5.

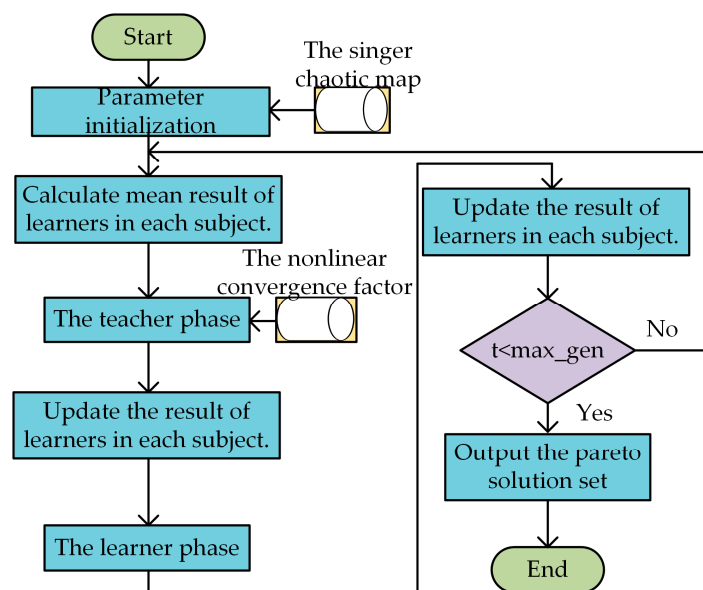


**Figure 5.** The flow chart of the ITLBO algorithm.

The content of the ITLBO algorithm is specifically explained based on the disassembly depth optimization problem of the EoL smartphones. The best solution (the optimal disassembly depth) is considered the teacher. All feasible disassembly depths are considered as the learners. The decision variables are the three factors in the objective function in Section 3.3. The search space is the value range of the above three factors. By analyzing the actual disassembly requirements of EoL smartphones, the range of the search space for disassembly profit per unit time should be greater than 0 and the range of the search space for the overall disassembly safety process rate should be greater than 70%. The implementation steps of the ITLBO are summarized as follows.

- (1) The parameter initialization. In order to avoid falling into local optimum, the singer chaotic map is used. The equation for the singer chaotic map [49] is determined as follows:

$$x_{k+1} = u \left( 7.86x_k - 23.31x_k^2 + 28.75x_k^3 - 13.302875x_k^4 \right), u \in (0.9, 1.08) \quad (22)$$

where  $x_k$  is the value of the  $k$ th singer chaotic map and  $u$  is the coefficient of the singer chaotic map.

- (2) The teacher phase. In this phase, learners learn through a teacher. In order to increase searchability and solution accuracy, the nonlinear convergence factor is used. The equation for the nonlinear convergence factor is determined as follows:

$$X_{\text{new}}^i = X_{\text{old}}^i + K(X_{\text{teacher}} - TF \cdot \text{Mean}) \quad (23)$$

$$TF = \frac{2}{\lg 2} \times \lg \left( 2 - \left( \frac{t}{t_{\max}} \right)^2 \right) \quad (24)$$

where  $X_{\text{new}}^i$  is the result of the  $i$ th learner after learning,  $X_{\text{old}}^i$  is the result of the  $i$ th student before learning,  $X_{\text{teacher}}$  is the result of the teacher,  $\text{Mean}$  is the mean of all learners,  $TF$  is the teaching factor,  $K$  is the random number in the range  $[0, 1]$ ,  $t$  is the current number of iterations and  $t_{\max}$  is the maximum number of iterations.

- (3) The learner phase. The learners increase their knowledge by interacting with each other. A learner interacts randomly with others to enhance their knowledge. The principle [50] is determined as follows:

$$X_N^i = \begin{cases} X^i + K(X^i - X^j), & T(X^j) < T(X^i) \\ X^i + K(X^j - X^i), & T(X^i) < T(X^j) \end{cases} \quad (25)$$

where  $X^i$  is the result for learner  $i$ ,  $X^j$  is the result for learner  $j$ ,  $X_N^i$  is the new result for learner  $i$  after the learner phase,  $T(X^i)$  is the fitness value of  $X^i$  and  $T(X^j)$  is the fitness value of  $X^j$ .

- (4) The pareto solution set. All non-inferior solutions of the disassembly depth are output. The pareto solution set can provide solutions for the multi-objective disassembly depth optimization problem of EoL smartphones.

### 3.5. The Assessment of Disassembly Depth

It is difficult to compare the advantages and disadvantages of the pareto solution in the solution set. For the disassembly problem, we should select the optimal disassembly depth. Fuzzy AHP is widely applied to address the uncertainty of decision-making and has been applied in many fields. Fuzzy AHP has obvious advantages in computational time, simplicity and stability. Therefore, fuzzy AHP is selected for assessment of the disassembly depth.

During the actual disassembling process, the disassembly time and the disassembly profit are considered to be the most important factors. The disassembly energy consumption is concerned with environmental protection issues. Moreover, the overall disassembly safety process should also be taken seriously. Therefore, disassembly time, disassembly energy consumption, disassembly profit and the overall safety of the disassembly process are selected as the criteria. The structural hierarchy of multi-objective disassembly depth decisions for EoL smartphones is shown in Figure 6. The fuzzy judgment matrix  $Q$  of the standard layers can be obtained as shown in Equation (26).

$$Q = \begin{pmatrix} q_{11} & q_{12} & q_{13} & q_{14} \\ q_{21} & q_{22} & q_{23} & q_{24} \\ q_{31} & q_{32} & q_{33} & q_{34} \\ q_{41} & q_{42} & q_{43} & q_{44} \end{pmatrix} \quad (26)$$

The elements of the fuzzy judgment matrix  $Q$  are determined based on the scale of the fuzzy AHP value. The 0.1–0.9 nine-level scale method is the maximum number of grades that people can accept. Thus, the 0.1–0.9 nine-level scale method is applied to the scale of the fuzzy AHP value. The weights of the criteria are determined based on the fuzzy judgment matrix  $Q$  and the specific steps are as follows.

Firstly, the fuzzy judgment matrix  $Q$  is summed by rows; the formula for its calculation is:

$$Q_y = \sum_{k=1}^{m_6} q_{yk} \quad (27)$$

where  $Q_y$  is the sum of row  $y$  of the fuzzy judgment matrix  $Q$  and  $m_6$  is the number of the criterion.

Then, the weight coefficient is calculated based on the following equation:

$$X_y = \frac{Q_y - 2 - m_6}{m_6(m_6 - 1)} \quad (28)$$

where  $X_y$  is the weight coefficient of row  $y$ .

Finally, the determinant of the weight coefficient  $ri$  is determined as follows:

$$ri = [X_1, X_2, \dots, X_{m_6}] \quad (29)$$

In order to verify whether the obtained weight is reliable, the fuzzy consistent matrix  $G$  is obtained. The specific treatment method is determined as follows:

$$G_{yk} = \frac{(m_6 - 1)(X_y - X_k)}{2} + 0.5 \quad (30)$$

$CI$  is calculated using the following equation. When  $CI < 0.1$ , it means that the data meets the requirements for fuzzy consistency. The average index for randomly generated weights  $R$  is set to 0.9 [15].

$$CI = \frac{\sum_{y=1}^{m_6} \sum_{k=1}^{m_6} |G_{yk} - q_{yk}|}{m_6^2 R} \quad (31)$$

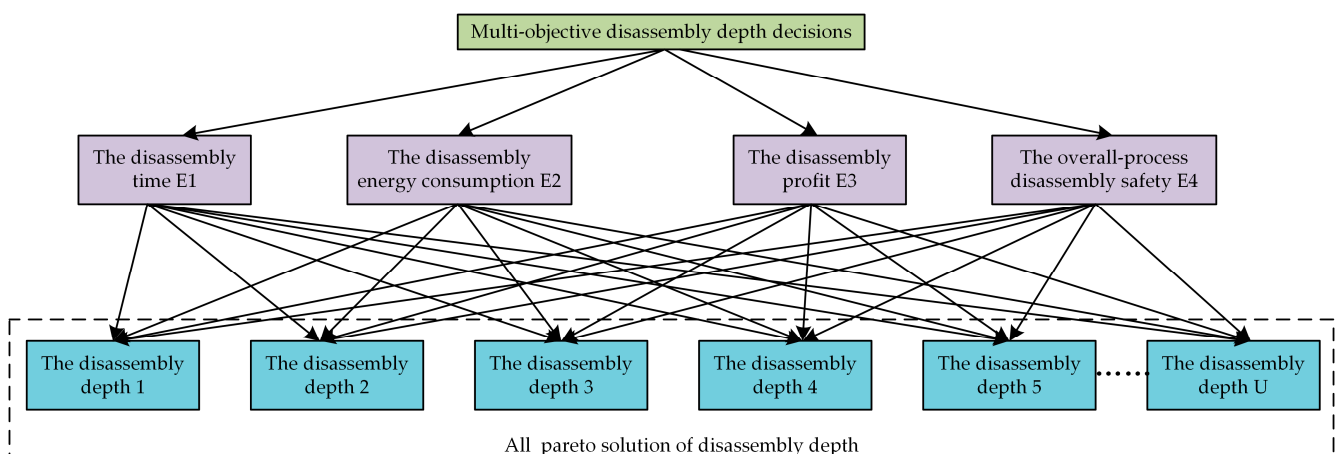


**Figure 6.** The structural hierarchy of multi-objective disassembly depth decisions.

## 4. Experiment and Discussion

### 4.1. Fundamental Data

The EoL smartphone, namely ‘Xiaomi 4’, was selected as an example to verify the applicability of the proposed method. The relevant information for ‘Xiaomi 4’ was obtained using the disassembly experiment. The disassembly parts graph for ‘Xiaomi 4’ is shown in Figure 7, and contains 11 main parts of ‘Xiaomi 4’ and their numbers. The precedence graph of ‘Xiaomi 4’, which shows the precedence constraint relationship between the 11 main parts of ‘Xiaomi 4’, is shown in Figure 8. In addition, the basic information for ‘Xiaomi 4’ is shown in Table 1. The disassembly tool information is shown in Table 2. In Table 1, the weight of the parts is measured using the electronic scale, and the recycling price for

parts is obtained through market research; the price of the parts may fluctuate. Because relative comparison is used in this study, the results of the study will not be affected by the recycling price of parts. In Table 2, the weight of the disassembly tool is measured using the electronic scale and the tool damage cost is estimated using the wholesale purchase prices and service life statistics. The wholesale purchase price and service life statistics are obtained through market research. The feasible disassembly depth of 'Xiaomi 4' is determined based on the precedence graph for 'Xiaomi 4', the basic information for 'Xiaomi 4' and the disassembly rules.



Figure 7. The disassembly parts graph for 'Xiaomi 4'.

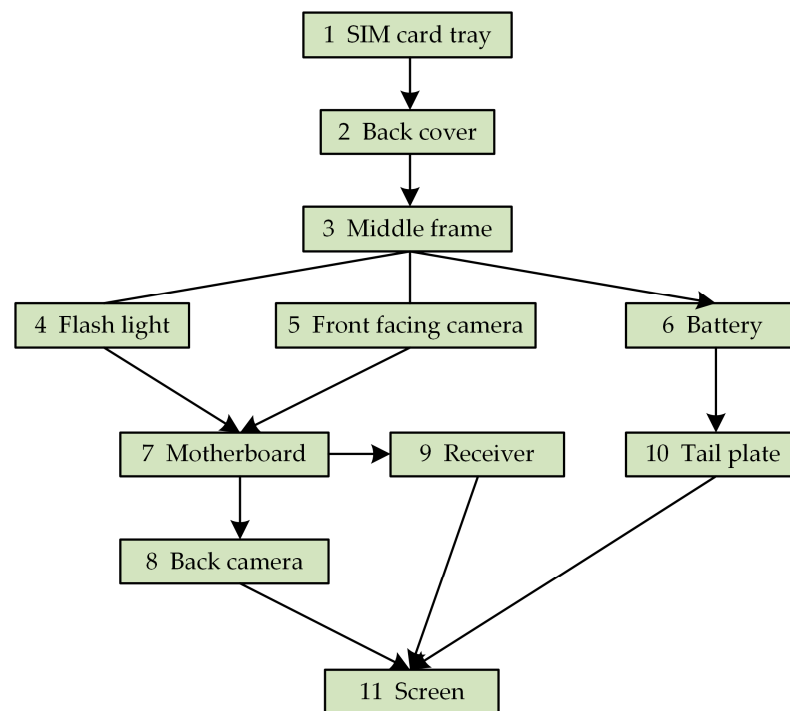


Figure 8. The precedence graph for 'Xiaomi 4'.

**Table 1.** The basic information for ‘Xiaomi 4’.

Part No.	Part Name	The Disassembly Direction	Constraint/Quantity	The Disassembly Tool	Weight (g)	The Basic Disassembly Time (s)	The Price (¥)
1	SIM card tray	+X	Buckle/1	Retrieve card pin	0.9	2.00	0.01
2	Back cover	+Z	Buckle/1	Stick–suction cups	11.2	15.50	0.80
3	Middle frame	+Z	Screws/10, buckle/1	Electric screwdriver– stick–tweezer	10.6	45.00	0.20
4	Flashlight	–Z	Screws/3	Electric screwdriver– tweezer	0.7	12.50	3.50
5	Front-facing camera	+Z	BTB/1	Stick–tweezer	0.3	6.00	15.00
6	Battery	+Z	BTB/1, sealant/1	Heating gun–stick–tweezer	46.0	65.00	11.50
7	Motherboard	+Z	Buckle/2	Stick–tweezer	14.1	16.00	45.00
8	Back camera	–Z	BTB/1	Stick–tweezer	0.7	8.00	22.00
9	Receiver	+Z	Buckle/1	Stick–tweezer	0.7	6.40	1.20
10	Tail plate	+Z	Sealant/1, screws/3	Electric screwdriver– Heating gun–tweezer	2.8	35.70	25.00
11	Screen	–Z	Sealant/1	Heating gun–tweezer–stick	62.6	80.00	1.30

**Table 2.** Disassembly tool information.

Tool Name	Weight (g)	Power (W)	The Tool Damage Cost for Each Use (¥)
Retrieve card pin	0.2	—	0.005
Electric screwdriver	248.1	50	0.01
Heating gun	210.6	300	0.01
Stick	18.6	—	0.01
Tweezer	12.8	—	0.002
Suction cups	2.1	—	0.005
Detector	—	5	—
Lamp	—	15	—

The disassembly time, the disassembly energy consumption, the disassembly profit and the overall safety of the disassembly process for each disassembly depth are calculated based on the established model. In order to improve the accuracy of the calculation, the quantitative parameters for ‘Xiaomi 4’ are shown in Table 3. The quantitative parameters for ‘Xiaomi 4’ are determined using the disassembly experiments and market research. Three operators with similar disassembly experiences are divided into groups A, B and C. The operator of every group disassembles the same part and repeats this 20 times (there are 20 experiments in each group). The number of risky disassembly experiments in every group is recorded. The risky disassembly probability for each part of ‘Xiaomi 4’ is shown in Table 4.

**Table 3.** The quantitative parameters of ‘Xiaomi 4’.

The Quantitative Parameters	Value	Unit	Data Source
The disassembly time for disassembling a screw	2.00	(s)	Disassembly experiments
The time required to change the disassembly tool once	3.00	(s)	
The tool positioning time	1.50	(s)	
The detection time for a part	7.00	(s)	
The tidying time for disassembling a part	4.50	(s)	
The heating time for disassembling the tail plate	15.00	(s)	
The heating time for disassembling the battery	45.00	(s)	
The heating time for disassembling the screen	55.00	(s)	
The weight of a screw	0.15	(g)	
The quality rate of recyclable parts	95.00%	—	
The recycling price of metal materials	4500.00	(¥·t <sup>-1</sup> )	
The recycling price of mixing materials	4000.00	(¥·t <sup>-1</sup> )	
The recycling price of plastic materials	2200.00	(¥·t <sup>-1</sup> )	
The purchase cost of EoL ‘Xiaomi 4’	35.00	(¥)	
The employee cost	32.00	(¥·h <sup>-1</sup> )	
The employee’s working time	8.00, 22.00	(h·d <sup>-1</sup> , d·m <sup>-1</sup> )	
The workshop rental cost	4000.00	(¥·m <sup>-1</sup> )	
The number of disassembly tables	10	—	
The price per kilowatt-hour of electricity	1.00	(¥·(kw·h) <sup>-1</sup> )	
The disassembly energy consumption for disassembling a screw	0.01	(J)	Disassembly experiments
The disassembly energy consumption for disassembling a BTB	0.03	(J)	
The disassembly energy consumption for disassembling a back cover	0.42	(J)	
Energy consumption for moving a part	11.50	(J)	
Energy consumption for moving a tool	15.00	(J)	
The disassembly energy consumption for disassembling a SIM card tray	0.03	(J)	
The disassembly energy consumption for disassembling a buckle	0.20	(J)	

**Table 4.** The risky disassembly probability of each part of ‘Xiaomi 4’.

Part No.	Group A		Group B		Group C		The Risky Disassembly Probability
	The Number of Risky Disassembly Experiments	The Number of Disassembly Experiments	The Number of Risky Disassembly Experiments	The Number of Disassembly Experiments	The Number of Risky Disassembly Experiments	The Number of Disassembly Experiments	
1	1	20	0	20	1	20	3.33%
2	0	20	1	20	1	20	3.33%
3	1	20	1	20	1	20	5.00%
4	0	20	1	20	0	20	1.67%
5	0	20	0	20	1	20	1.67%
6	1	20	2	20	1	20	6.67%
7	1	20	0	20	1	20	3.33%
8	0	20	1	20	0	20	1.67%
9	1	20	1	20	0	20	3.33%
10	1	20	1	20	1	20	5.00%
11	2	20	2	20	1	20	8.33%

#### 4.2. Results

The program is developed using Matlab2019b and its running environment is Intel® coreli7@2.3GHZ, RAM16.00Gn, win7 system. Based on the practicability of disassembly, the population size is set to 15 and the iteration number is set to 100. The disassembly depth non-inferior solution set for ‘Xiaomi 4’ is obtained as shown in Table 5. In order to show the results in Table 5 intuitively, the spatial distribution of the non-inferior solution is shown in Figure 9. The number in Figure 9 corresponds to the number of disassembly depths in Table 5.

Table 5. The disassembly depth non-inferior solution set for ‘Xiaomi 4’.

Disassembly Depth No.	Disassembly Depth	Disassembly Profit per unit Time (¥·t <sup>-1</sup> )	Disassembly Energy Consumption per Unit Time (J·t <sup>-1</sup> )	The Overall Disassembly Safety Process Rate
1	1-2-3-5-6-10-4-7-8	0.1854	63.3579	72.3439%
2	1-2-3-5-4-7	0.1024	22.3968	82.9795%
3	1-2-3-5-4-7-8	0.1688	21.8929	81.5937%
4	1-2-3-5-4-7-8-9	0.1565	21.5224	78.8767%
5	1-2-3-5-4-7-9-8	0.1565	21.5224	78.8767%
6	1-2-3-4-5-7	0.1024	22.3968	82.9795%
7	1-2-3-4-5-7-8	0.1688	21.8929	81.5937%
8	1-2-3-4-5-7-8-9	0.1565	21.5224	78.8767%

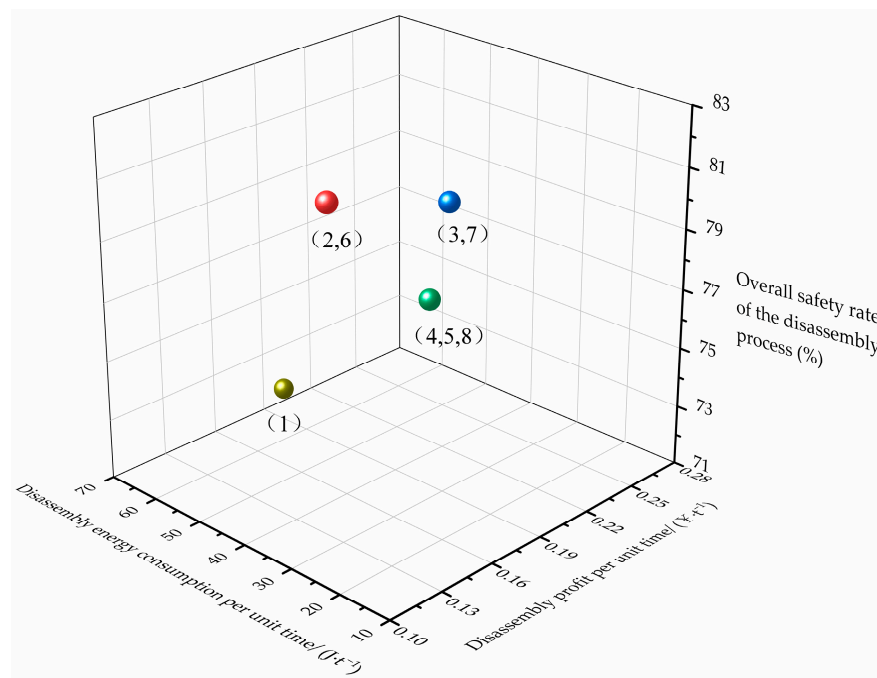


Figure 9. The spatial distribution of the non-inferior solution.

Based on the four criteria, the fuzzy judgment matrix *Q* of the standard layers can be obtained as shown in Table 6. The method used to obtain the values in Table 6 is as follows: three researchers with disassembly experience compared the importance of all evaluation indexes at the same level and got consistent results. The values in Table 6 were then assigned according to the assignment criteria of the 0.1–0.9 nine-level scale method. The results of the weight coefficients and the *CI* are shown in Table 7. Due to the degree of inconsistency within the allowable range (*CI* = 0.09805 < 0.1), the result of this decision is credible. The weights of the impact of each criterion on each scheme are synthesized and the relevant information on data processing is shown in Table 8. By analyzing the comprehensive sort of Table 8, the optimal disassembly depth for ‘Xiaomi 4’ is disassembly depth 3 (SIM card tray–Back cover–Middle frame–Front-facing camera–Flashlight–Motherboard–Back camera) and disassembly depth 7 (SIM card tray–Back cover–Middle frame–Flashlight–Front-facing camera–Motherboard–Back camera).

**Table 6.** The fuzzy judgment matrix  $Q$  of the standard layers.

Criteria	E <sub>1</sub>	E <sub>2</sub>	E <sub>3</sub>	E <sub>4</sub>
E <sub>1</sub>	0.5	0.2	0.6	0.3
E <sub>2</sub>	0.8	0.5	0.7	0.6
E <sub>3</sub>	0.4	0.3	0.5	0.4
E <sub>4</sub>	0.7	0.4	0.6	0.5

**Table 7.** The results of the weight coefficient and the CI.

Criteria	Weights	
E <sub>1</sub>	0.2167	CI = 0.09805
E <sub>2</sub>	0.3	
E <sub>3</sub>	0.2167	
E <sub>4</sub>	0.2667	

**Table 8.** The weighted decision data.

	Criteria	E <sub>1</sub>	E <sub>2</sub>	E <sub>3</sub>	E <sub>4</sub>	Comprehensive Sort
	Weight	0.2167	0.3	0.2167	0.2667	
Pareto solution	Disassembly depth 1	0.1018	0.0929	0.15	0.1018	0.1095
	Disassembly depth 2	0.15	0.1125	0.1071	0.1446	0.1280
	Disassembly depth 3	0.1304	0.1268	0.1357	0.1304	0.1305
	Disassembly depth 4	0.1125	0.1429	0.1214	0.1161	0.1245
	Disassembly depth 5	0.1125	0.1429	0.1214	0.1161	0.1245
	Disassembly depth 6	0.15	0.1125	0.1071	0.1446	0.1280
	Disassembly depth 7	0.1304	0.1268	0.1357	0.1304	0.1305
	Disassembly depth 8	0.1089	0.1429	0.1214	0.1161	0.1237

#### 4.3. Analysis of Results and Discussion

In order to verify the applicability of the method proposed in this paper, the existing disassembly depth optimization methods in [39,40] were selected for comparison. In the experiment, the disassembly depth optimization method in [39] (select the disassembly depth with the maximum total disassembly profit in all disassembly depths) is set as group A. The disassembly depth optimization method in [40] (select the disassembly depth with a maximum total disassembly profit of more than 85% and maximum total disassembly energy consumption of less than 70% in all disassembly depths) is set as group B. The disassembly depth optimization method proposed in this paper is set as group C. The disassembly depth optimization results of 'Xiaomi 4' are shown in Table 9.

The number of non-inferior solutions is increased by eight in group C compared with the results in group A. The number of optimal solutions is increased by two in group C compared with the results in group A. The results of the comparison demonstrate that the searchability of the non-inferior solution and the optimal solution is improved in group C compared with the results in group A. Compared with the results in group B, the number of non-inferior solutions is increased by seven in group C. Compared with the results in group B, the number of optimal solutions is increased by two in group C. The results of the comparison show that group C is better than group B at improving the searchability of the non-inferior solution and the optimal solution. In summary, the searchability of the non-inferior solution and the optimal solution of the method proposed in this paper is superior to the methods in [39,40].

In order to verify the applicability of the ITLBO algorithm in this paper, the existing TLBO algorithm is selected for comparison. The EoL smartphone 'Xiaomi 4' is selected as the case. The parameters of the ITLBO algorithm and the TLBO algorithm are set to the same value (the population size is set to 15 and the iteration number is set to 100). The disassembly profit per unit time, the disassembly energy consumption per unit time and the overall safety rate of the disassembly process are selected as optimization objectives. Each

algorithm is iterated 10 times. Figure 10 shows the relationship between the average value of the minimum disassembly energy consumption per unit time and the iteration number of the program. Figure 11 shows the relationship between the average value of the maximum disassembly profit per unit of time and the iteration number of the program. Figure 12 shows the relationship between the average value of the maximum overall disassembly safety rate and the iteration number of the program.

**Table 9.** The disassembly depth optimization results for ‘Xiaomi 4’.

Group	The Disassembly Depth	The non-Inferior Solution	The Optimal Solution	Disassembly Profit per Unit Time (¥·t <sup>-1</sup> )	Disassembly Energy Consumption per unit Time (J·t <sup>-1</sup> )	The overall Disassembly Safety Process Rate
A	1-2-3-5-6-10-4-7-8-9	×	×	0.1764	60.6200	69.94%
B	1-2-3-5-6-10-4-7-8	✓	×	0.1854	63.3579	72.3439%
	1-2-3-5-6-10-4-7-8-9	×	×	0.1764	60.6200	69.94%
	1-2-3-5-6-10-4-7-9-8	×	×	0.1764	60.6200	69.94%
	1-2-3-5-4-7-8-9-6-10	×	×	0.1764	60.6200	69.94%
	1-2-3-5-4-7-9-8-6-10	×	×	0.1764	60.6200	69.94%
	1-2-3-4-5-7-8-9-6-10	×	×	0.1764	60.6200	69.94%
C	1-2-3-5-6-10-4-7-8	✓	×	0.1854	63.3579	72.3439%
	1-2-3-5-4-7	✓	×	0.1024	22.3968	82.9795%
	1-2-3-5-4-7-8	✓	✓	0.1688	21.8929	81.5937%
	1-2-3-5-4-7-8-9	✓	×	0.1565	21.5224	78.8767%
	1-2-3-5-4-7-9-8	✓	×	0.1565	21.5224	78.8767%
	1-2-3-4-5-7	✓	×	0.1024	22.3968	82.9795%
	1-2-3-4-5-7-8	✓	✓	0.1688	21.8929	81.5937%
	1-2-3-4-5-7-8-9	✓	×	0.1565	21.5224	78.8767%

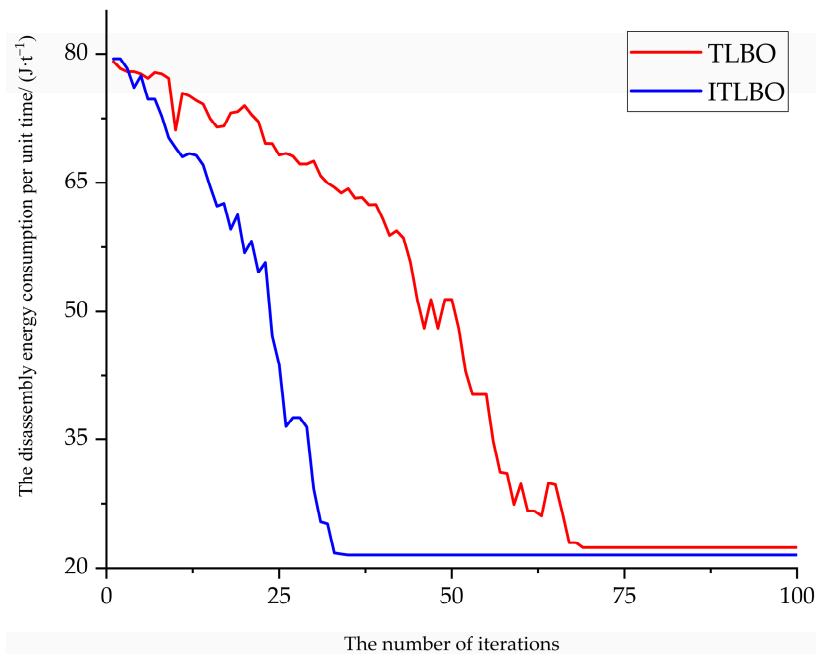


**Figure 10.** The average value of the minimum disassembly energy consumption per unit of time versus the number of iterations.

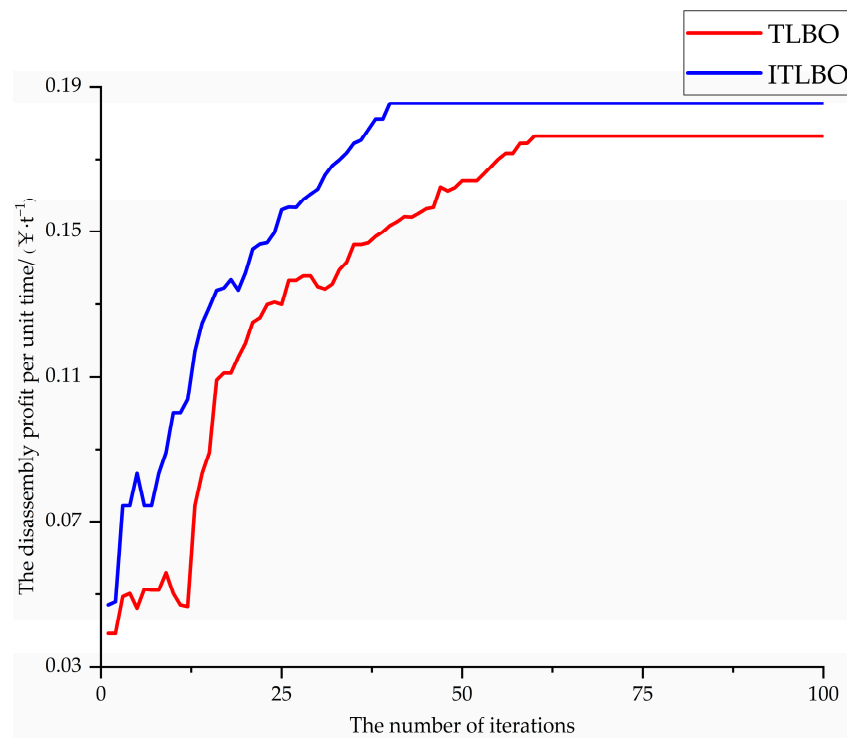


**Figure 11.** The average value of the maximum disassembly profit per unit time versus the number of iterations.

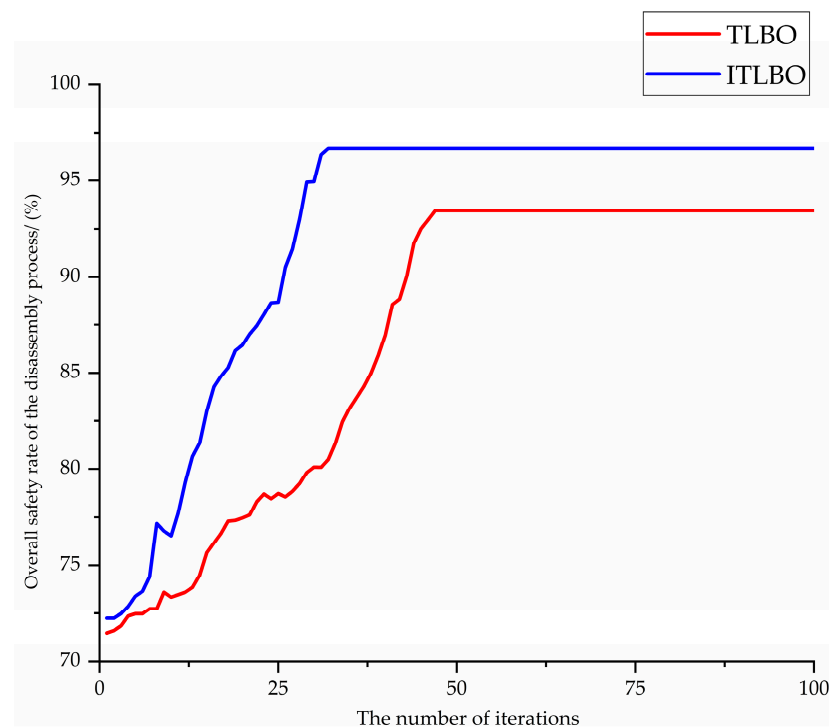


**Figure 12.** The average value of the maximum overall safety rate of the disassembly process versus the number of iterations.

During the process of searching for the optimal disassembly energy consumption per unit time, it can be seen from Figure 10 that the ITLBO algorithm tends to converge in the 35th generation, while the TLBO algorithm tends to converge in the 70th generation. Compared with the TLBO algorithm, the convergence speed of the ITLBO algorithm is increased by 50.00%. Moreover, it can be seen from Figure 10 that the minimum disassembly

energy consumption per unit time obtained by the TLBO algorithm is  $22.3968 \text{ J}\cdot\text{t}^{-1}$ , while the minimum disassembly energy consumption per unit time obtained by the ITLBO algorithm is  $21.5224 \text{ J}\cdot\text{t}^{-1}$ . Compared with the TLBO algorithm, the minimum disassembly energy consumption per unit time by the ITLBO algorithm is reduced by 3.91%.

In the process of searching for the optimal disassembly profit per unit time, it can be seen from Figure 11 that the ITLBO algorithm tends to converge in the 40th generation, while the TLBO algorithm tends to converge in the 60th generation. Compared with the TLBO algorithm, the convergence speed of the ITLBO algorithm increased by 33.33%. Moreover, it can be seen from Figure 11 that the maximum disassembly profit per unit time obtained by the TLBO algorithm is  $0.1764 \text{ ¥}\cdot\text{t}^{-1}$ , while the maximum disassembly profit per unit time obtained by the ITLBO algorithm is  $0.1854 \text{ ¥}\cdot\text{t}^{-1}$ . Compared with the TLBO algorithm, the maximum disassembly profit per unit of time obtained by the ITLBO algorithm increased by 5.10%.

In the process of searching for the optimal overall safety rate of the disassembly process, it can be seen from Figure 12 that the ITLBO algorithm tends to converge in the 32nd generation, while the TLBO algorithm tends to converge in the 46th generation. Compared with the TLBO algorithm, the convergence speed of the ITLBO algorithm increased by 30.43%. Moreover, it can be seen from Figure 12 that the maximum overall disassembly safety rate obtained by the TLBO algorithm is 93.45%, while the maximum overall disassembly safety rate obtained by the ITLBO algorithm is 96.67%. Compared with the TLBO algorithm, the maximum overall disassembly safety rate of the ITLBO algorithm increased by 3.45%. In summary, the convergence speed and solution accuracy of the ITLBO algorithm are superior to those of the TLBO algorithm.

From the case study and the above analysis, the proposed method can effectively determine the optimal disassembly depth of EoL smartphones. Although we have successfully applied the proposed method to EoL smartphones, there are some limitations to this proposed method. Firstly, we assume that the disassembly is in an ideal state and the parts are not damaged during the disassembly process. In order to obtain more accurate results, it is important to reasonably consider the damage rate during the disassembly process. Then, it is important to choose a more reasonable criterion for fuzzy AHP for the EoL smartphones. Moreover, an EoL smartphone, namely 'Xiaomi 4', was selected as an example of multiple waste electronic products in this paper. In order to prove the effectiveness and high utilization rate of the method, it is important to study other old equipment to determine the application range for the proposed method.

## 5. Conclusions

With the explosion in the number of waste electrical and electronic equipment, it is particularly important to reduce the influence of electrical and electronic equipment waste via disassembly planning. One of the most crucial domains within disassembly research is the intricate challenge of securing a satisfactory disassembly depth. Unfortunately, the overall disassembly safety process is not considered in the disassembly depth optimization process, which leads to an inability to accurately obtain a reasonable disassembly depth. Therefore, a multi-objective disassembly depth optimization method for EoL smartphones, considering the overall safety of the disassembly process, is proposed. In this study, a multi-objective function for disassembly depth optimization of EoL smartphones is established based on disassembly profit per unit time, disassembly energy consumption per unit time and overall disassembly safety process rate. In order to increase the solution accuracy and avoid local optimization, an improved teaching–learning-based optimization algorithm is proposed. The overall disassembly safety process, disassembly time, disassembly energy consumption and disassembly profit are selected as the criteria for fuzzy AHP to obtain the optimal disassembly depth for EoL smartphones. A case of the 'Xiaomi 4' is studied to verify the applicability of the proposed method. The key observations obtained from the results of the experiments can be summarized as follows.

- (a) The numbers of non-inferior solutions and optimal solutions obtained using the method proposed in this paper are superior to the methods in [39,40]. The searchability of the non-inferior solution and the optimal solution of the method proposed in this paper is significant.
- (b) In the process of searching for the optimal objective, the convergence speeds for the ITLBO algorithm were 50.00%, 33.33% and 30.43% higher than for the TLBO algorithm. This shows that the ITLBO algorithm is more effective than the TLBO algorithm at improving the convergence speed when searching for the optimal objective.
- (c) In the process of searching for the optimal objective, the optimal solution values of the ITLBO algorithm were 3.91%, 5.10% and 3.45% higher than for the TLBO algorithm. This shows that the ITLBO algorithm is more effective than the TLBO algorithm at improving the solution accuracy of searching for the optimal objective.

This paper is only a preliminary exploration of multi-objective disassembly depth optimization problems for EoL smartphones, considering the overall safety of the disassembly process. Further research is needed on carbon dioxide emissions and the disassembly damage rate of the disassembly process. Optimizing the disassembly depth based on the disassembly workshop is a future research direction.

**Author Contributions:** Conceptualization, Z.C., L.L. and X.C.; methodology, Z.C. and L.L.; software, Z.C.; validation, Z.C.; formal analysis, L.L., F.Y. and H.L.; investigation, L.L., X.C., F.Y. and H.L.; resources, X.C. and F.Y.; data curation, L.L., X.C., F.Y. and H.L.; writing—original draft preparation, Z.C.; writing—review and editing, L.L. and F.Y.; supervision, L.L. and F.Y.; project administration, L.L. and F.Y.; funding acquisition, L.L. All authors have read and agreed to the published version of the manuscript.

**Funding:** This work was supported by the National Key Research and Development Program of China (grant number 2020YFB1713001).

**Institutional Review Board Statement:** Not applicable.

**Informed Consent Statement:** Not applicable.

**Data Availability Statement:** Data will be made available on request.

**Acknowledgments:** The authors would like to express their sincere gratitude to the anonymous reviewers for their many valuable comments and suggestions.

**Conflicts of Interest:** The authors declare no conflicts of interest. The funders had no role in the design of the study; in the collection, analyses, or interpretation of data; in the writing of the manuscript; or in the decision to publish the results.

## References

1. Zeng, Y.; Zhang, Z.; Yin, T.; Zheng, H. Robotic disassembly line balancing and sequencing problem considering energy-saving and high-profit for waste household appliances. *J. Clean. Prod.* **2022**, *381*, 135209. [[CrossRef](#)]
2. He, P.; Wang, C.; Zuo, L. The present and future availability of high-tech minerals in waste mobile phones: Evidence from China. *J. Clean. Prod.* **2018**, *192*, 940–949. [[CrossRef](#)]
3. Li, J.; Ge, Z.; Liang, C.; An, N. Present status of recycling waste mobile phones in China: A review. *Environ. Sci. Pollut. Res.* **2017**, *24*, 16578–16591. [[CrossRef](#)] [[PubMed](#)]
4. Ren, Y.; Jin, H.; Zhao, F.; Qu, T.; Meng, L.; Zhang, C.; Zhang, B.; Wang, G.; Sutherland, J.W. A multi-objective disassembly planning for value recovery and energy conservation from end-of-life products. *IEEE Trans. Autom. Sci. Eng.* **2021**, *18*, 791–803. [[CrossRef](#)]
5. Nowakowski, P. A novel, cost efficient identification method for disassembly planning of waste electrical and electronic equipment. *J. Clean. Prod.* **2018**, *172*, 2695–2707. [[CrossRef](#)]
6. Paterson, D.A.P.; Ijomah, W.L.; Windmill, J.F.C. End-of-life decision tool with emphasis on remanufacturing. *J. Clean. Prod.* **2017**, *148*, 653–664. [[CrossRef](#)]
7. Wang, K.; Li, X.; Gao, L. Modeling and optimization of multi-objective partial disassembly line balancing problem considering hazard and profit. *J. Clean. Prod.* **2019**, *211*, 115–133. [[CrossRef](#)]
8. Bentaha, M.L.; Dolgui, A.; Battaia, O.; Riggs, R.J.; Hu, J. Profit-oriented partial disassembly line design: Dealing with hazardous parts and task processing times uncertainty. *Int. J. Prod. Res.* **2018**, *56*, 7220–7242. [[CrossRef](#)]

9. Cordella, M.; Alfieri, F.; Clemm, C.; Berwald, A. Durability of smartphones: A technical analysis of reliability and repairability aspects. *J. Clean. Prod.* **2021**, *286*, 125388. [[CrossRef](#)]
10. Islam, M.T.; Dias, P.R.; Huda, N. Waste mobile phones: A survey and analysis of the awareness, consumption and disposal behavior of consumers in Australia. *J. Environ. Manage.* **2020**, *275*, 111111. [[CrossRef](#)]
11. Ren, Y.; Zhang, C.; Zhao, F.; Tian, G.; Lin, W.; Meng, L.; Li, H. Disassembly line balancing problem using interdependent weights-based multi-criteria decision making and 2-Optimal algorithm. *J. Clean. Prod.* **2018**, *174*, 1475–1486. [[CrossRef](#)]
12. Liu, J.; Zhou, Z.; Pham, D.T.; Xu, W.; Ji, C.; Liu, Q. Collaborative optimization of robotic disassembly sequence planning and robotic disassembly line balancing problem using improved discrete Bees algorithm in remanufacturing. *Robot. Comput. Integr. Manuf.* **2020**, *61*, 101829. [[CrossRef](#)]
13. Ren, Y.; Yu, D.; Zhang, C.; Tian, G.; Meng, L.; Zhou, X. An improved gravitational search algorithm for profit-oriented partial disassembly line balancing problem. *Int. J. Prod. Res.* **2017**, *55*, 7302–7316. [[CrossRef](#)]
14. Mandolini, M.; Favi, C.; Germani, M.; Marconi, M. Time-based disassembly method: How to assess the best disassembly sequence and time of target components in complex products. *Int. J. Adv. Manuf. Technol.* **2018**, *95*, 409–430. [[CrossRef](#)]
15. Yang, Y.; Yuan, G.; Zhuang, Q.; Tian, G. Multi-objective low-carbon disassembly line balancing for agricultural machinery using MDFOA and fuzzy AHP. *J. Clean. Prod.* **2019**, *233*, 1465–1474. [[CrossRef](#)]
16. Cao, J.; Xia, X.; Wang, L.; Zhang, Z.; Liu, X. A Novel Multi-Efficiency Optimization Method for Disassembly Line Balancing Problem. *Sustainability* **2019**, *11*, 6969. [[CrossRef](#)]
17. Lu, Q.; Ren, Y.; Jin, H.; Meng, L.; Li, L.; Zhang, C.; Sutherland, J.W. A hybrid metaheuristic algorithm for a profit-oriented and energy-efficient disassembly sequencing problem. *Robot. Comput. Integr. Manuf.* **2020**, *61*, 101828. [[CrossRef](#)]
18. Xu, W.; Tang, Q.; Liu, J.; Liu, Z.; Zhou, Z.; Pham, D.T. Disassembly sequence planning using discrete Bees algorithm for human-robot collaboration in remanufacturing. *Robot. Comput. Integr. Manuf.* **2020**, *62*, 101860. [[CrossRef](#)]
19. Xing, Y.; Wu, D.; Qu, L. Parallel disassembly sequence planning using improved ant colony algorithm. *Int. J. Adv. Manuf. Technol.* **2021**, *113*, 2327–2342. [[CrossRef](#)]
20. Liu, H.; Zhang, L. Optimizing a disassembly sequence planning with success rates of disassembly operations via a variable neighborhood search algorithm. *IEEE Access* **2021**, *9*, 157540–157549. [[CrossRef](#)]
21. Liang, J.; Guo, S.; Zhang, Y.; Liu, W.; Zhou, S. Energy-efficient optimization of two-sided disassembly line balance considering parallel operation and uncertain using multiobjective flatworm algorithm. *Sustainability* **2021**, *13*, 3358. [[CrossRef](#)]
22. Aicha, M.; Belhadj, I.; Hammadi, M.; Aifaoui, N. A mathematical formulation for processing time computing in disassembly lines and its optimization. *Comput. Ind. Eng.* **2022**, *165*, 107933. [[CrossRef](#)]
23. Zeng, Y.; Zhang, Z.; Liang, W.; Zhang, Y. Balancing optimization for disassembly line of mixed homogeneous products with hybrid disassembly mode. *Comput. Ind. Eng.* **2023**, *185*, 109646. [[CrossRef](#)]
24. Wang, K.; Guo, J.; Du, B.; Li, Y.; Tang, H.; Li, X.; Gao, L. A novel MILP model and an improved genetic algorithm for disassembly line balancing and sequence planning with partial destructive mode. *Comput. Ind. Eng.* **2023**, *186*, 109704. [[CrossRef](#)]
25. Yeh, W.C. Optimization of the disassembly sequencing problem on the basis of self-adaptive simplified swarm optimization. *IEEE Trans. Syst. Man. Cybern.-Part. A Syst. Hum.* **2011**, *42*, 250–261. [[CrossRef](#)]
26. Xia, K.; Gao, L.; Li, W.; Chao, K. Disassembly sequence planning using a simplified teaching-learning-based optimization algorithm. *Adv. Eng. Inform.* **2014**, *28*, 518–527. [[CrossRef](#)]
27. Tseng, H.E.; Chang, C.C.; Lee, S.C.; Huang, Y.M. A block-based genetic algorithm for disassembly sequence planning. *Expert. Syst. Appl.* **2018**, *96*, 492–505. [[CrossRef](#)]
28. Xie, J.; Li, X.; Gao, L. Disassembly sequence planning based on a modified grey wolf optimizer. *Int. J. Adv. Manuf. Technol.* **2021**, *116*, 3731–3750. [[CrossRef](#)]
29. Tseng, H.E.; Huang, Y.M.; Chang, C.C.; Lee, S.C. Disassembly sequence planning using a Flatworm algorithm. *J. Manuf. Syst.* **2020**, *57*, 416–428. [[CrossRef](#)]
30. Tseng, H.E.; Chang, C.C.; Chung, T.W. Applying improved particle swarm optimization to asynchronous parallel disassembly planning. *IEEE Access* **2022**, *10*, 80555–80564. [[CrossRef](#)]
31. Lou, S.; Zhang, Y.; Tan, R.; Lv, C. A human-cyber-physical system enabled sequential disassembly planning approach for a human-robot collaboration cell in Industry 5.0. *Robot. Comput. Integr. Manuf.* **2024**, *87*, 102706. [[CrossRef](#)]
32. Kalayci, C.B.; Polat, O.; Gupta, S.M. A hybrid genetic algorithm for sequence-dependent disassembly line balancing problem. *Ann. Oper. Res.* **2016**, *242*, 321–354. [[CrossRef](#)]
33. Liu, J.; Wang, S. Balancing disassembly line in product recovery to promote the coordinated development of economy and environment. *Sustainability* **2017**, *9*, 309. [[CrossRef](#)]
34. Liu, J.; Sang, H.; Han, Y.; Wang, C.; Gao, K. Efficient multi-objective optimization algorithm for hybrid flow shop scheduling problems with setup energy consumptions. *J. Clean. Prod.* **2018**, *181*, 584–598. [[CrossRef](#)]
35. Xia, X.; Liu, W.; Zhang, Z.; Wang, L.; Cao, J.; Liu, X. A Balancing Method of Mixed-model Disassembly Line in Random Working Environment. *Sustainability* **2019**, *11*, 2304. [[CrossRef](#)]
36. Xu, W.; Cui, J.; Liu, B.; Liu, J.; Yao, B.; Zhou, Z. Human-robot collaborative disassembly line balancing considering the safe strategy in remanufacturing. *J. Clean. Prod.* **2021**, *324*, 129158. [[CrossRef](#)]
37. Liang, P.; Fu, Y.; Gao, K. Multi-product disassembly line balancing optimization method for high disassembly profit and low energy consumption with noise pollution constraints. *Eng. Appl. Artif. Intell.* **2024**, *130*, 107721. [[CrossRef](#)]

38. Giudice, F.; Kassem, M. End-of-life impact reduction through analysis and redistribution of disassembly depth: A case study in electronic device redesign. *Comput. Ind. Eng.* **2009**, *57*, 677–690. [[CrossRef](#)]
39. Achillas, C.; Aidonis, D.; Vlachokostas, C.; Karagiannidis, A.; Moussiopoulos, N.; Loulos, V. Depth of manual dismantling analysis: A cost–benefit approach. *Waste Manag.* **2013**, *33*, 948–956. [[CrossRef](#)] [[PubMed](#)]
40. Smith, S.; Hsu, L.; Smith, G.C. Partial disassembly sequence planning based on cost-benefit analysis. *J. Clean. Prod.* **2016**, *139*, 729–739. [[CrossRef](#)]
41. Kubler, S.; Robert, J.; Derigent, W.; Voisin, A.; Traon, Y.L. A state-of the-art survey & testbed of fuzzy AHP (FAHP) applications. *Expert. Syst. Appl.* **2016**, *65*, 398–422.
42. Liu, Y.; Eckert, C.M.; Earl, C. A review of fuzzy AHP methods for decision-making with subjective judgements. *Expert. Syst. Appl.* **2020**, *161*, 113738. [[CrossRef](#)]
43. Heo, E.; Kim, J.; Boo, K.J. Analysis of the assessment factors for renewable energy dissemination program evaluation using fuzzy AHP. *Renew. Sust. Energ. Rev.* **2010**, *14*, 2214–2220. [[CrossRef](#)]
44. Avikal, S.; Jain, R.; Mishra, P.K. A Kano model, AHP and M-TOPSIS method-based technique for disassembly line balancing under fuzzy environment. *Appl. Soft Comput.* **2014**, *25*, 519–529. [[CrossRef](#)]
45. Guler, D.; Yomralioglu, T. Suitable location selection for the electric vehicle fast charging station with AHP and fuzzy AHP methods using GIS. *Ann. GIS* **2020**, *26*, 169–189. [[CrossRef](#)]
46. Zhou, X.; Sun, Y.; Huang, Z.; Yang, C.; Yen, G.G. Dynamic multi-objective optimization and fuzzy AHP for copper removal process of zinc hydrometallurgy. *Appl. Soft Comput.* **2022**, *129*, 109613. [[CrossRef](#)]
47. Sherif, S.U.; Asokan, P.; Sasikumar, P.; Mathiyazhagan, K.; Jerald, J. An integrated decision making approach for the selection of battery recycling plant location under sustainable environment. *J. Clean. Prod.* **2022**, *330*, 129784. [[CrossRef](#)]
48. Tuo, Y.; Zhang, Z.; Wu, T.; Zeng, Y.; Zhang, Y.; Junqi, L. Multimanned disassembly line balancing optimization considering walking workers and task evaluation indicators. *J. Manuf. Syst.* **2024**, *72*, 263–286. [[CrossRef](#)]
49. Oliva, D.; Abd El Aziz, M.; Hassanien, A.E. Parameter estimation of photovoltaic cells using an improved chaotic whale optimization algorithm. *Appl. Energy* **2017**, *200*, 141–154. [[CrossRef](#)]
50. Baykasoğlu, A.; Hamzadayi, A.; Köse, S.Y. Testing the performance of teaching–learning based optimization (TLBO) algorithm on combinatorial problems: Flow shop and job shop scheduling cases. *Inf. Sci.* **2014**, *276*, 204–218. [[CrossRef](#)]

**Disclaimer/Publisher’s Note:** The statements, opinions and data contained in all publications are solely those of the individual author(s) and contributor(s) and not of MDPI and/or the editor(s). MDPI and/or the editor(s) disclaim responsibility for any injury to people or property resulting from any ideas, methods, instructions or products referred to in the content.